Eur. Phys. J. A **14**, 255–263 (2002)
DOI 10.1140/epja/i2002-10002-4

THE EUROPEAN PHYSICAL JOURNAL A

Probing the interactions of charmed mesons with nuclei in p̄-induced reactions

Ye.S. Golubeva[1], W. Cassing[2,a], and L.A. Kondratyuk[3]

[1] Institute for Nuclear Research, 60th October Anniversary Prospect 7A, 117312 Moscow, Russia
[2] Institut für Theoretische Physik, Universität Giessen, D-35392 Giessen, Germany
[3] Institute of Theoretical and Experimental Physics, B. Cheremushkinskaya 25, 117259 Moscow, Russia

Received: 1 March 2002
Communicated by V.V. Anisovich

Abstract. We study the perspectives of resonant and nonresonant charmed-meson production in $\bar{p}+A$ reactions within the Multiple Scattering Monte Carlo (MSMC) approach. We calculate the production of the resonances $\Psi(3770), \Psi(4040)$ and $\Psi(4160)$ on various nuclei, their propagation and decay to $D, \bar{D}, D^*, \bar{D}^*, D_s, \bar{D}_s$ in the medium and vacuum, respectively. The modifications of the open charm vector mesons in the nuclear medium are found to be rather moderate or even small such that dilepton spectroscopy will require an invariant mass resolution of a few MeV. Furthermore, the elastic and inelastic interactions of the open charm mesons in the medium are taken into account, which can be related to (u,d)-, s- or c-quark exchange with nucleons. It is found that by studying the $D/\bar{D}$ ratio for low momenta in the laboratory ($\leq 2-2.2$ GeV/c) as a function of the target mass A stringent constraints on the c-quark exchange cross-section can be obtained. On the other hand, the ratios D_s^-/D_s^+ as well as D/D_s^- and D/D_s^+ at low momenta as a function of A will permit to fix independently the strength of the s-quark exchange reaction in $D_s^- N$ scattering.

PACS. 25.43.+t Antiproton-induced reactions – 14.40.Lb Charmed mesons – 14.65.Dw Charmed quarks – 13.25.Ft Decays of charmed mesons

1 Introduction

In the last decade the dynamics of charm quark degrees of freedom have gained sizeable interest especially in the context of a phase transition to the quark-gluon plasma (QGP) where charmed-meson states should no longer be formed due to color screening [1–5]. However, the suppression of the $c\bar{c}$ vector mesons in the high-density phase of nucleus-nucleus collisions might also be attributed to inelastic comover scattering (cf. [6–9] and refs. therein) if the corresponding charmonium-hadron cross-sections are of the order of a few mb [10,11]. Also the $J/\Psi N$ cross-section is not known sufficiently well [12] since the photoproduction data suggest a value of 3–4 mb [13], while the charmonium absorption on nucleons (at high relative momentum) in $p+A$ and $A+A$ reactions is conventionally fitted by 6–7 mb [9,14] which might relate to the cross-section of a pre-resonance charmonium state with nucleons before the actual hadronic state is formed. Present estimates for the J/Ψ formation times range from 0.3–0.5 fm/c [13], but additional data from $\bar{p}$-induced reactions on nuclei, where charmonium can be formed on resonance with moderate momenta relative to the target nucleons, should help to pin down the present uncertainties [15]. Such studies might be performed experimentally at the HESR, which is presently proposed as a future facility at GSI [16].

In a previous study we have explored the perspectives of charmed meson-nucleon scattering in the $\bar{p}d$ reaction [17] where the charmonium is produced on resonance with the proton in the deuteron and may scatter with the spectator neutron. Another possibility is also the reaction $\pi^+ d \to J/\psi pp$ as discussed by Brodsky and Miller in ref. [18]. Here we investigate $\bar{p}A$ reactions and study the production of the resonances $\Psi(3770), \Psi(4040)$ and $\Psi(4160)$ in various nuclei, their propagation and decay to $D, \bar{D}, D^*, \bar{D}^*, D_s, \bar{D}_s$ in the medium and vacuum, respectively. Furthermore, the elastic and inelastic interactions of the open charm mesons in the medium are followed up in the Multiple Scattering Monte Carlo (MSMC) approach to study the dominant medium effects as a function of the target mass A.

Our work is organized as follows: In sect. 2 we will briefly describe the MSMC approach and evaluate the formation cross-sections for the resonances $\Psi(3770), \Psi(4040)$ and $\Psi(4160)$ on protons and nuclei. The fractional decay

[a] e-mail: Wolfgang.Cassing@theo.physik.uni-giessen.de

of these resonances to open charm mesons in the medium and vacuum, respectively, is calculated in sect. 3 whereas the dynamics of the open charm mesons is described and studied in sect. 4. Section 5 concludes this paper with a summary and discussion of open problems.

2 Resonance production and decay in $\bar{p}p$ and $\bar{p}A$ reactions

We here examine the possibility to measure the in-medium lifetime (or total width) of the resonances $V = (\Psi(3770), \Psi(4040)\, \Psi(4160))$ produced in $\bar{p}A$ reactions. Before doing so one has to determine first the resonance properties in vacuum, *i.e.* their production in $\bar{p}p$ reactions. To this aim we describe the vector meson spectral function by a Breit-Wigner distribution

$$A_V(M^2) = N_V \frac{M\Gamma^V_{\rm tot}(M)}{(M^2 - M_V^2 - \Re\Pi_V(M))^2 + M^2\Gamma^2_{\rm tot}(M)}, \tag{1}$$

where M_V denotes the vacuum pole mass, $\Re\Pi_V$ is the vector meson self-energy in the medium —which vanishes in the vacuum— and $N_V \sim 1/\pi$ (for small width $\Gamma_{\rm tot}$) is a normalization factor that ensures $\int {\rm d}M^2 A(M^2) = 1$. The total width $\Gamma_{\rm tot}$ is separated into vacuum and medium contributions as

$$\Gamma_{\rm tot}(M) = \Gamma_{\rm vac}(M) + \Gamma_{\rm coll}(M), \tag{2}$$

where

$$\Gamma_{\rm vac}(M) = \sum_c \Gamma_c(M) \tag{3}$$

with $\Gamma_c(M)$ denoting the partial width to the decay channels $c \equiv D\bar{D},\ D\bar{D}^*,\ D^*\bar{D},\ D^*\bar{D}^*,\ D_s\bar{D}_s,\ D_s^*\bar{D}_s,\ D_s\bar{D}_s^*,\ D_s^*\bar{D}_s^*$, respectively. The in-medium collisional width is determined from the imaginary part of the forward vector-meson nucleon scattering amplitude as

$$\Gamma_{\rm coll} = \frac{4\pi}{M} \Im f_V(0) \rho_A, \tag{4}$$

where ρ_A denotes the nuclear density. Furthermore, $\Im f_V(0)$ is determined via the optical theorem by the total vector-meson nucleon cross-section σ_{VN} that will be specified below. The real part of the vector meson self-energy $\Re\Pi_V(M)$ in the medium might be calculated by dispersion relations, however, QCD sum rules for $c\bar{c}$ vector states suggest that the "mass shift" $\Re\Pi/(2M_V)$ at normal nuclear matter density is only of the order of a few MeV [19] due to a small coupling of the $c, \bar{c}$ quarks to the nuclear medium. We thus will assume $\Re\Pi_V = 0$ throughout the following study.

2.1 Vacuum properties

Whereas the pole masses of the vector mesons M_V are approximately known, *e.g.*, from e^+e^- annihilation [20] this does not hold for the total widths and especially branching ratios. To this end, we have to model the vacuum decays, that enter the spectral function (1) via (3), using available information from the PDG [21]. In each channel c the relative decay to mesons m_1 and m_2 is described by a matrix element (squared) and phase space, *i.e.*

$$\Gamma_c \sim |\mathcal{M}_c|^2 p_c^3, \tag{5}$$

where p_c is the meson momentum in the rest frame of the resonance. In case of the $\Psi(3770)$ only the lowest channel to $D\bar{D}$ contributes such that the matrix element in (5) can be fixed by the total width at half maximum which we take as $\Gamma_{\rm FWHM} = 25$ MeV [21]. For the $\Psi(4040)$ and $\Psi(4160)$ we adopt $\Gamma_{\rm FWHM} = 50$ MeV and $\Gamma_{\rm FWHM} = 80$ MeV, respectively [21]. The branching ratios for the $\Psi(4040)$ show a strong anomaly favoring the decays to channels with vector mesons D^*. The PDG [21] quotes $\Gamma(D^0\bar{D}^0)/\Gamma(D^{*0}\bar{D}^0 + {\rm c.c.}) = 0.05 \pm 0.03$ and $\Gamma(D^{*0}\bar{D}^{*0})/\Gamma(D^{*0}\bar{D}^0 + {\rm c.c.}) = 32 \pm 12$, where the phase space factor $\sim p_c^3$ already has been divided out. The origin for such a large variation in the matrix elements is not known so far. We use the actual numbers (within the range of uncertainty)

$$\frac{\mathcal{M}^2_{D\bar{D}}}{\mathcal{M}^2_{D^*\bar{D}}} = 0.08;\ \frac{\mathcal{M}^2_{D^*\bar{D}^*}}{\mathcal{M}^2_{D^*\bar{D}}} = 22;$$

$$\frac{\mathcal{M}^2_{D\bar{D}}}{\mathcal{M}^2_{D_s\bar{D}_s}} = 3;\ \frac{\mathcal{M}^2_{D_s\bar{D}_s^*}}{\mathcal{M}^2_{D_s\bar{D}_s}} = 12.5;\ \frac{\mathcal{M}^2_{D_s^*\bar{D}_s^*}}{\mathcal{M}^2_{D_s\bar{D}_s^*}} = 22, \tag{6}$$

that provide a reasonable description to the e^+e^- formation data from ref. [20]. The resulting spectral function $S(M) = 2MA(M)$ for the $\Psi(4040)$ (with a pole mass of 4.08 GeV) is shown in fig. 1 (upper part) in terms of the thick solid line as well as the mass-dependent branching ratios for the different channels c (including the phase space factor $\sim p_c^3$). It is clearly seen that for the ratios (6) the $D^*\bar{D}^*$ decay opens up at $M \approx 4.03$ GeV and dominates the spectral function for higher masses. Furthermore, the decays to D_s, D_s^* are strongly suppressed such that this resonance does not qualify for the production of $(s\bar{c})$ or $(c\bar{s})$ mesons.

Apart from the total width of 80 $\pm$25 MeV the properties of the $\Psi(4160)$ are not well known experimentally. For the decay channels we thus adopt a "counting rule" for high-energy open charm production that results from PYTHIA calculations (cf. fig. 1 in ref. [22]), *i.e.*

$$\frac{\mathcal{M}^2_{D\bar{D}}}{\mathcal{M}^2_{D^*\bar{D}}} = \frac{1}{3};\ \frac{\mathcal{M}^2_{D^*\bar{D}^*}}{\mathcal{M}^2_{D^*\bar{D}}} = 3;\ \frac{\mathcal{M}^2_{D\bar{D}}}{\mathcal{M}^2_{D_s\bar{D}_s}} = 3;$$

$$\frac{\mathcal{M}^2_{D_s\bar{D}_s^*}}{\mathcal{M}^2_{D_s\bar{D}_s}} = 3;\ \frac{\mathcal{M}^2_{D_s^*\bar{D}_s^*}}{\mathcal{M}^2_{D_s\bar{D}_s^*}} = 3. \tag{7}$$

This is presently nothing but an educated guess (at low energies) and must be controlled by future data. The resulting spectral function $S(M) = 2MA(M)$ for the $\Psi(4160)$ is shown in fig. 1 (lower part) in terms of the thick solid line as well as the mass-dependent branching ratios for the

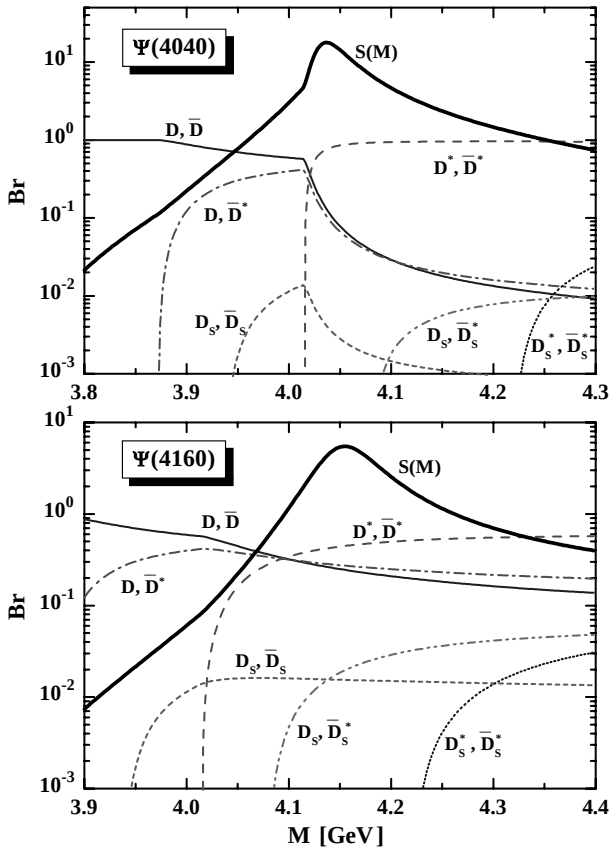

Fig. 1. The spectral functions $S(M)$ for the $\Psi(4040)$ and $\Psi(4160)$ (thick lines, not normalized) and the mass differential branching ratios for both vector mesons within the model described in the text.

different channels c. It is clearly seen that for the ratios (7) the $D^*\bar{D}^*$ decay still dominates the spectral function, however, the decays to D_s, D_s^* are no longer so strongly suppressed as in case of the $\Psi(4040)$.

The production of the vector mesons in $\bar{p}p$, then, can be described by the Breit-Wigner resonance formation on the basis of the spectral function $A(M^2)$ (1) —employing the proper kinematics— provided that the branching of $\bar{p}p \to V$ is known,

$$\sigma_V(M) = \frac{3}{4}\mathrm{Br}_{p\bar{p}\to V} 4MA_V(M)\Gamma_V^{\mathrm{tot}}(M)\frac{\pi^2}{k^2}, \qquad (8)$$

where the factor 3/4 stems from the ratio of spin factors and k denotes the momentum of the p (or $\bar{p}$) in the cms. In fact, the branching ratio is rather uncertain for the cases of interest here. Following our previous work [17] we adopt $\mathrm{Br}(p\bar{p} \to \Psi(3770)) \approx 2 \times 10^{-4}$ which is very similar to the branching of the $\Psi(2S)$ state. Due to a lack of detailed knowledge we assume this branching ratio also to hold for the $\Psi(4040)$ and $\Psi(4160)$. The resulting cross-sections for the mesons V in $\bar{p}p$ reactions are displayed in fig. 2 (upper part) as a function of the antiproton kinetic energy $T_{\bar{p}}$ in the laboratory reflecting the resonance structure (1) and the kinematics from (8).

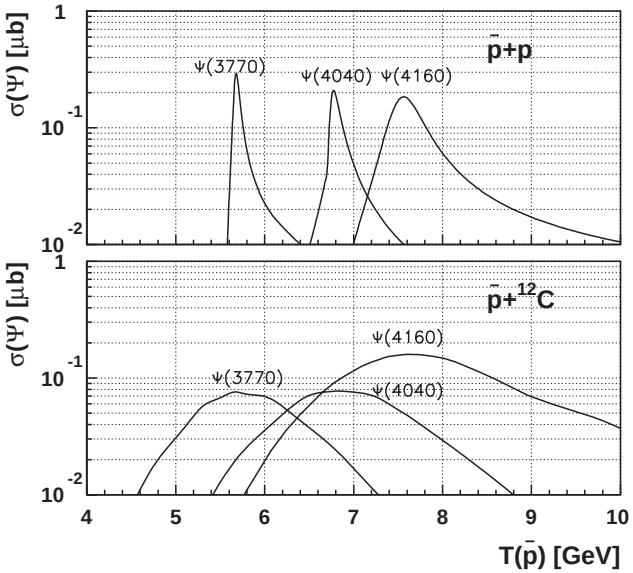

Fig. 2. The calculated cross-sections for $\Psi(3770)$, $\Psi(4040)$ and $\Psi(4160)$ for $\bar{p}p$ (upper part) and $\bar{p}+{}^{12}$C reactions (lower part) as a function of the antiproton kinetic energy in the laboratory.

2.2 p̄A reactions

In order to simulate events for the reaction $\bar{p}A \to V$ we use the Multiple Scattering Monte Carlo (MSMC) approach. An earlier version of this approach —denoted as Intra-Nuclear Cascade (INC) model— has been applied to the analysis of η and ω production in $\bar{p}A$ and pA interactions in refs. [23–26]. The production of the hidden charm vector resonances on nuclei then can be evaluated within the MSMC by propagating the antiproton in the nucleus and folding the elementary $\bar{p}p \to V$ production cross-section with the local momentum distribution at the annihilation point. We have calculated the latter quantity in the local Thomas-Fermi approximation.

The numerical results for the formation cross-sections of the resonances V on ^{12}C are shown in the lower part of fig. 2 as a function of $T_{\bar{p}}$ indicating that the resonance formation is further smeared out by Fermi motion and the maximum in the cross-section becomes reduced inspite of the larger $\bar{p}$ annihilation cross-section on ^{12}C. The suppression factor in the maximum of the cross-section —per elementary reaction— is of the order (see ref. [27])

$$\mathrm{S.F.} \simeq \frac{\pi\Gamma_R m_N}{(k_{\mathrm{F}} M_R)}, \qquad (9)$$

where Γ_R, M_R denote the vacuum width and mass of the produced meson, whereas k_{F} is the target Fermi momentum. This leads to factors of ~ 0.075, 0.14 and 0.21 for $\Psi(3770), \Psi(4040)$ and $\Psi(4160)$ per $p\bar{p}$ reaction, respectively. On the other hand, the production on nuclei roughly scales with the target proton number as $Z^{0.6}$ (see below) such that the cross-section for ^{12}C in the maximum for the $\Psi(4160)$ is roughly the same as in $\bar{p}p$ annihilation, while it is lower for the narrower resonances $\Psi(3770)$ and $\Psi(4040)$.

Necessary parameters for a Monte Carlo (MC) simulation of rescattering are the elastic and inelastic VN scattering cross-sections and slope parameters b for the differential cross-sections $\mathrm{d}\sigma_{\mathrm{el}}/\mathrm{d}t$, which are approximated by

$$\frac{\mathrm{d}\sigma_{\mathrm{el}}}{\mathrm{d}t} \sim \exp(bt), \tag{10}$$

where t is the momentum transfer squared. These parameters as well as the masses of the rescattered particles determine the momentum and angular distributions of the particles in the final state. As in our previous study [17] we use $b = 1\ \mathrm{GeV}^{-2}$ for $D, \bar{D}$+N and VN scattering as an educated guess. Furthermore, the inelastic cross-sections of the vector mesons with nucleons have to be specified. Since the relative momenta in the V-N system for rescattering are of the order of a few GeV one might use high-energy geometric cross-sections for the dissociation to open charm mesons. For all the three resonances studied here we adopt an inelastic cross-section of 11 mb as well as $\sigma_{\mathrm{el}} = 1\,\mathrm{mb}$. The inelastic cross-section of 11 mb is larger by about a factor of 2 in comparison to the $J/\Psi, \Psi(2S)$ cross-sections (see introduction) due to the larger size of the higher-lying resonances.

As mentioned above, the resonances V are propagated without any mean-field potential. This approximation should be well fulfilled since the expected potentials are only of the order of a few MeV [19] while the energy of vector mesons in the laboratory frame is a couple of GeV. Furthermore, due to the high mass of the resonances we neglect any intrinsic formation time τ_{F} for the resonances.

The resonances are propagated with their actual mass M —selected by MC according to the spectral function (1)— with velocity p_V/E_V and decay in time according to the differential equation

$$\frac{\mathrm{d}P_V}{\mathrm{d}t} = -\frac{1}{\gamma}\Gamma^V_{\mathrm{tot}}(M)P_V(t) \tag{11}$$

with the total width (2), while γ denotes the Lorentz γ-factor. Their decay to $D\bar{D}$, $D\bar{D}^*$, $D^*\bar{D}$, $D^*\bar{D}^*$, $D_s\bar{D}_s$, $D_s^*\bar{D}_s$, $D_s\bar{D}_s^*$, $D_s^*\bar{D}_s^*$ is, furthermore, selected by Monte Carlo according to the mass differential branching ratios displayed in fig. 1.

Due to the rather moderate collision rates involved (for $\sigma^{\mathrm{tot}}_{VN} \approx 12\,\mathrm{mb}$) the lifetime of the vector mesons $\Psi(3770), \Psi(4040)$ and $\Psi(4160)$ is not reduced sizeably in the nuclear medium relative to the vacuum (assuming the open charm mesons not to change their properties in the medium). This reduction then amounts to about 15% for the $\Psi(3770)$, to $\sim 8\%$ for the $\Psi(4040)$ and to $\sim 5\%$ for the $\Psi(4160)$, respectively. On the other hand, the $D, \bar{D}$ mesons might change their effective mass in the nuclear medium as advocated in refs. [28–30]. Especially for dropping $D, \bar{D}$ effective masses in the medium the decay width of the vector mesons becomes enhanced at finite density ρ_A. This effect is most pronounced for the $\Psi(3770)$ since its pole mass is close to the $D, \bar{D}$ threshold of ~ 3.73 GeV. A drop of the $D, \bar{D}$ meson masses both by 50 MeV at density ρ_0 would imply an increase of the decay width by about a factor of 2.5 according to phase space. Thus in-medium modifications of the open charm mesons might alter the lifetime of the $\Psi(3770)$ more effectively than collisional broadening. However, in-medium potentials are most pronounced at low momenta and decrease in size with increasing momentum. Thus it is very questionable if $D, \bar{D}$ mesons will have sizeable potentials for relative momenta of 3–5 GeV/c with respect to the nucleus at rest. Thus, in the following, we do not speculate any further on such medium mass modifications of $D, \bar{D}$ mesons at high relative momentum and continue our calculations for vacuum properties of the open charm system.

The open charm mesons from the decaying vector mesons have a light quark $q = (u, d)$ or strange s-quark content apart from the $\bar{c}$- or c-quark. In the constituent quark model we get $D^+ = (c\bar{d})$, $D^- = (\bar{c}d)$, $\bar{D}^0 = (\bar{c}u)$, $D^0 = (c\bar{u})$, $D_s^+ = (c\bar{s})$, $D_s^- = (\bar{c}s)$ and the same composition for the related vector states. Now light-quark exchanges with nucleons ((uud) or (udd)) have different strength as is well established experimentally from K^+p and K^-p reactions. Whereas the $K^+(u\bar{s})$ scatters only elastically with nucleons at low momentum —since the $\bar{s}$ cannot be exchanged with a light quark of a nucleon— the $K^-(s\bar{u})$ cross-section is dominated by resonant s-quark transfer leading to strange baryons such as Λ or Σ hyperons. Similar relations are expected to hold for the $D, \bar{D}$ mesons, where especially the light-quark contribution should give much larger cross-section on nucleons than the $c\bar{c}$ vector resonances. This analogy is based on $SU(4)_{\mathrm{flavor}}$ symmetry [31] which, however, might be broken substantially in view of the different geometrical sizes of K- and D-mesons. At present this is an open question, which has to be settled by experiment.

For our calculations we adopt the following cross-sections —taken as constants in the momentum regime of interest—

$$\begin{aligned} \sigma^{\mathrm{el}}_{DN} = \sigma^{\mathrm{el}}_{\bar{D}N} &= 10\,\mathrm{mb}; \\ \sigma^{\mathrm{inel}}_{\bar{D}N} \approx 0; \qquad \sigma^{\mathrm{inel}}_{DN} &= 10\,\mathrm{mb}; \\ \sigma^{\mathrm{el}}_{D_sN} = \sigma^{\mathrm{el}}_{\bar{D}_sN} &= 3\,\mathrm{mb}; \\ \sigma^{\mathrm{inel}}_{D_s^+N} \approx 3\,\mathrm{mb}; \qquad \sigma^{\mathrm{inel}}_{D_s^-N} &= 10\,\mathrm{mb}. \end{aligned} \tag{12}$$

Here the inelastic cross-sections of D-mesons refer to c-quark exchange reactions with nucleons. Furthermore, charge exchange reactions like $D^+n \leftrightarrow D^0p$ or $D^-p \leftrightarrow \bar{D}^0n$ are incorporated with a constant cross-section $\sigma_{q\,\mathrm{exc.}} = 12$ mb. For our exploratory study we assume the same cross-sections for the related open charm vector mesons $D^*, \bar{D}^*$ etc.

3 Resonance production in p̄A reactions

Within the model described in sect. 2 we are now in the position to calculate the cross-section of the $c\bar{c}$ resonances in $\bar{p}A$ reactions for all targets of interest and can obtain the information about in-medium resonance decays (for densities $\rho_A \geq 0.03\,\mathrm{fm}^{-3}$) or vacuum decays, respectively. In this respect we show in fig. 3 the calculated cross-section for the $\Psi(3770)$ at $T_{\mathrm{lab}} = 5.7$ GeV for the targets ^{12}C,

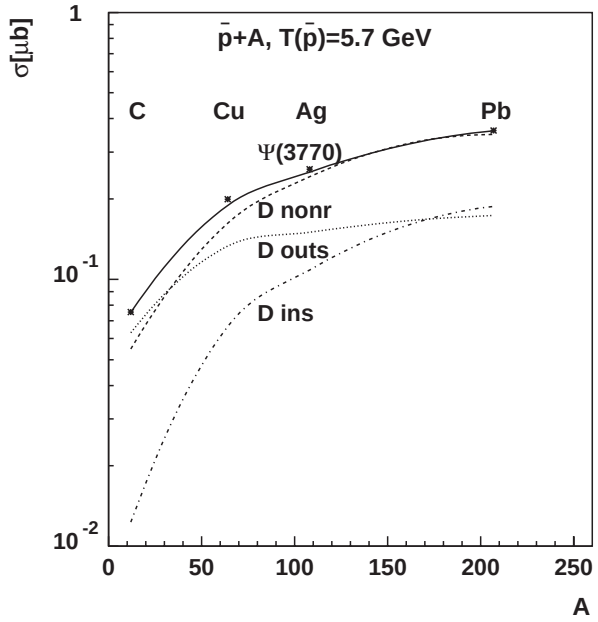

Fig. 3. The calculated cross-sections for $\Psi(3770)$ at $T_{\rm lab} = 5.7$ GeV as a function of the target mass A. The dotted line (D outs) denotes the contribution from "outside" resonance decays, whereas the dash-dotted line (D ins) shows the resonance contribution from "inside" decays. The solid line reflects the scaling law (13) for $\alpha = 0.55$ for the total contribution from the resonance decay. The dashed line (D nonr) corresponds to the estimated nonresonant $D, \bar{D}$ cross-section.

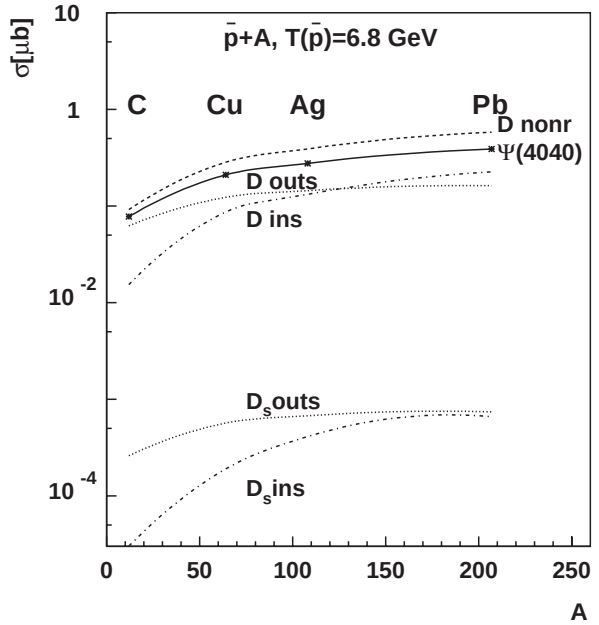

Fig. 4. The calculated cross-sections for $\Psi(4040)$ at $T_{\rm lab} = 6.8$ GeV as a function of the target mass A. The dotted line (D outs) denotes the contribution from "outside" resonance decays whereas the dash-dotted line (D ins) shows the resonance contribution from "inside" decays. The solid line reflects the sum of "outside" and "inside" resonance decay contributions. The dashed line (D nonr) corresponds to the estimated nonresonant $D, \bar{D}$ cross-section. The lower two lines give the "outside" and "inside" decay to $D_s, \bar{D}_s$, respectively.

^{64}Cu, ^{108}Ag and ^{207}Pb as a function of the target mass A. The solid line represents the power law

$$\sigma_\Psi \sim A^\alpha \tag{13}$$

with $\alpha = 0.55$, which nicely describes the total $\Psi(3770)$ yield. The coefficient α is less than $2/3$ —as expected from the total $\bar{p}$ annihilation cross-section— due to fact that only reactions with protons can lead to uncharged resonances and the Fermi smearing is more effective in heavy than in light nuclei. The fraction of $\Psi(3770)$, that decay to $D\bar{D}$ inside the nucleus (D ins) is only a few % in case of the ^{12}C target, however, reaches about 50% for the Pb target. Thus for a heavy target the in-medium properties of the $\Psi(3770)$ may well be studied experimentally by dilepton spectroscopy exploiting the dilepton branching of 7×10^{-4} of this resonance. However, as mentioned above, a collisional broadening of its spectral function by $\sim 15\%$ is not expected to provide a clear signal relative to its vacuum decay unless the experimental mass resolution is of the order of 1-2 MeV.

Apart from the resonant production of open charm mesons they may also be produced directly as $(c\bar{q})$ and $(\bar{c}q)$ pairs in $\bar{p}N$ annihilation. This channel strongly dominates in annihilation reactions on neutrons in the nucleus since the charmonium production is forbidden by charge conservation at low energy above threshold. At higher invariant energies a pion might balance the charge in the $\Psi + \pi$ final channel. For our estimates we have employed the Regge-model analysis of ref. [32] for the elementary $\bar{p}N \to D, \bar{D}$ cross-section as also used by Sibirtsev *et al.* in refs. [28,29]. The resulting cross-section of nonresonant open charm production is shown in fig. 3 as a function of the target mass A in terms of the dashed line (D nonr) and demonstrates that the nonresonant cross-section is about the same at this energy as the resonant production channel via $\Psi(3770)$ production and decay. Thus, in-medium modifications of the $\Psi(3770)$ will be hard to detect experimentally via the $D\bar{D}$ invariant mass spectrum (see below).

In analogy to fig. 3 we show in figs. 4 and 5 the calculated cross-section for the $\Psi(4040)$ at $T_{\rm lab} = 6.8$ GeV and $\Psi(4160)$ at $T_{\rm lab} = 7.7$ GeV for the targets ^{12}C, ^{64}Cu, ^{108}Ag and ^{207}Pb as a function of the target mass A. Due to the shorter lifetimes of these resonances the fraction of in-medium resonance decays increases up to 65% and 75%, respectively, for a Pb target. However, for the rescattering cross-sections involved (cf. sect. 2) the lifetimes in the medium are shortened only by 8% and 5%, respectively. This very moderate change of the spectral functions due to in-medium interactions will be hard to see by dilepton spectroscopy except for setups with excellent invariant mass resolution.

For the $\Psi(4040)$ the nonresonant $D, \bar{D}$ cross-section (upper dashed line; D nonr) becomes larger than the resonant cross-section (solid line) due to the higher invariant energy $\sqrt{s}$ involved in the elementary reactions at $T_{\rm lab} = 6.8$ GeV. Furthermore, the resonant decays to $D_s, \bar{D}_s$ are suppressed by almost 3 orders of magni-

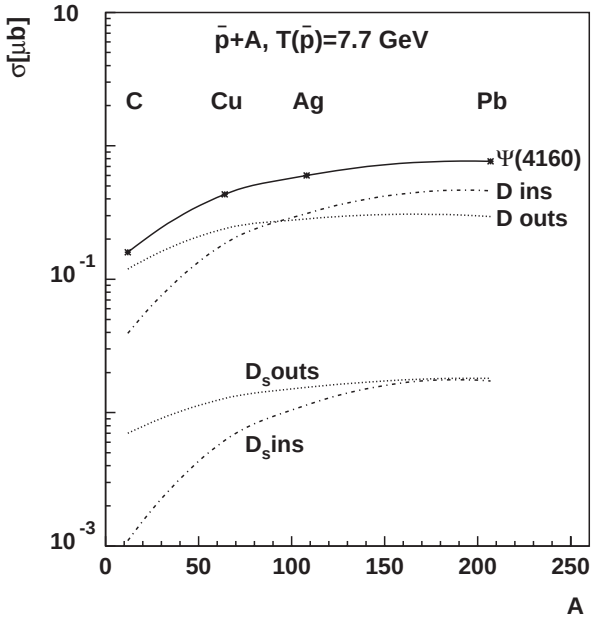

Fig. 5. The calculated cross-sections for $\Psi(4160)$ at $T_{\rm lab} = 7.7$ GeV as a function of the target mass A. The dotted line (D outs) denotes the contribution from "outside" resonance decays whereas the dash-dotted line (D ins) shows the resonance contribution from "inside" decays. The solid line reflects the sum of "outside" and "inside" resonance decay contributions. The lower two lines give the "outside" and "inside" decay to $D_s, \bar{D}_s$, respectively.

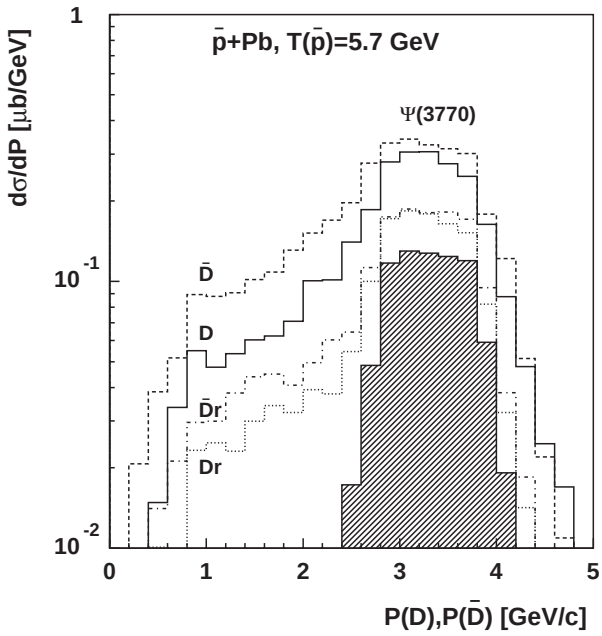

Fig. 6. The calculated momentum distributions of $D, \bar{D}$ mesons for $\bar{p}$ + Pb reactions at $T_{\rm lab} = 5.7$ GeV. The hatched area reflects open charm mesons from $\Psi(3770)$ decays in vacuum, the dotted (Dr) and dash-dotted ($\bar{\rm D}$r) lines correspond to resonance decays in the target nucleus, respectively. The solid and dashed lines display the total spectra for D- and $\bar{D}$-mesons including the nonresonant production channels (see text). In the calculations elastic and inelastic scatterings of the $\Psi(3770)$ and $D, \bar{D}$ mesons have been taken into account.

tude in case of the $\Psi(4040)$ which is not favorable for studying the $D_s, \bar{D}_s$ propagation in the nuclear medium. For the $\Psi(4160)$ an even larger nonresonant contribution is expected which we do not attempt to estimate explicitly since no educated guess for the additional channels $\bar{D}D\pi + X$ is available. However, the perspectives for $D_s, \bar{D}_s$ dynamics become more promising due to larger branching ratios which are a consequence of the higher invariant energy above the threshold and a more favorable matrix element. Especially for the heaviest targets almost 50% of the $D_s, \bar{D}_s$ mesons from $\Psi(4160)$ decay appear inside the nucleus such that rescattering effects can be explored. Such rescattering phenomena can also be tested for nonresonant $D_s, \bar{D}_s$ production channels; however, their cross-section is (at present) hard to estimate as mentioned before.

4 Open charm propagation and rescattering

The open charm mesons produced by resonance decay or nonresonant channels may rescatter in the nuclear medium either elastically or inelastically. In case of inelastic reaction channels there may be charge exchange reactions such as $D^+n \leftrightarrow D^0p$ or $\bar{D}^-p \leftrightarrow \bar{D}^0n$ or charm flavor exchange reactions $DN \to \Lambda_c\pi$ or $\Sigma_c\pi$ in analogy to the strangeness exchange reactions $\bar{K}N \to \Lambda\pi$ or $\Sigma\pi$. Whereas charge exchange reactions —induced by (u, d) quark exchange— do not change the ratio $D/\bar{D}$ in nuclei, the charm exchange reaction leads to a loss of c-quarks in the mesonic sector and thus to a decrease of the $D/\bar{D}$ ratio with the target mass number A.

In order to obtain some idea about the momenta of open charm mesons in the laboratory we display in fig. 6 the momentum distribution of D- and $\bar{D}$-mesons —after full rescattering— for $\bar{p}$ + Pb at $T_{\rm lab} = 5.7$ GeV. At this energy the resonance contribution stems from the $\Psi(3770)$; its "outside" decay contribution is shown in fig. 6 by the hatched area, which extends from 2.2 GeV/c to about 4.2 GeV/c. The "inside" resonance contribution (denoted by $\bar{\rm D}$r and Dr, respectively) is seen to be broadened significantly by elastic scattering and charge exchange reactions showing also a sizeable net absorption of D-mesons in case of the Pb target of $\sim 30\%$. On the other hand, the $D, \bar{D}$ mesons from nonresonant production channels signal larger in-medium rescattering effects which is seen by comparison to the total D (solid line) and $\bar{D}$ (dashed line) momentum spectra. The latter phenomenon is due to the fact that rescattering of open charm mesons in case of nonresonant production channels may proceed earlier than in case of the $\Psi(3770) \to D\bar{D}$ channel since the $\Psi(3770)$ on average is propagating for a couple of fm/c before its decay.

In order to quantify the observable consequences from $D, \bar{D}$ rescattering and absorption we have made a cut on the laboratory momenta $P_D, P_{\bar{D}} \leq 2.2$ GeV/c to exclude the vacuum decays of the $\Psi(3770)$ and to reduce

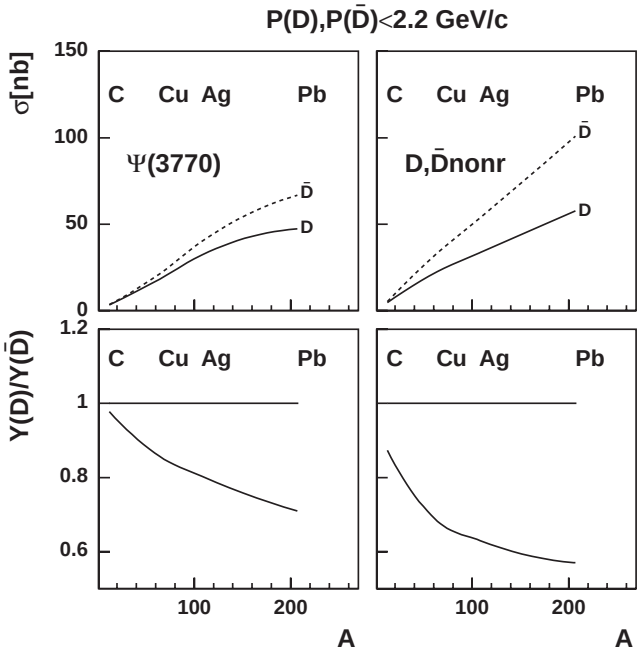

Fig. 7. Upper part: The calculated cross-sections for D- and $\bar{D}$-mesons for $\bar{p} + A$ reactions at $T_{\rm lab} = 5.7$ GeV including a low-momentum cut P_D, $P_{\bar{D}} \leq 2.2$ GeV/c. The l.h.s. shows the contribution from in-medium resonance decays whereas the r.h.s. corresponds to nonresonant production channels. Lower part: The ratio $D/\bar{D}$ *versus* the target mass A for resonant (l.h.s.) and nonresonant (r.h.s.) production channels. The constant line (= 1) results when neglecting c-quark exchange channels.

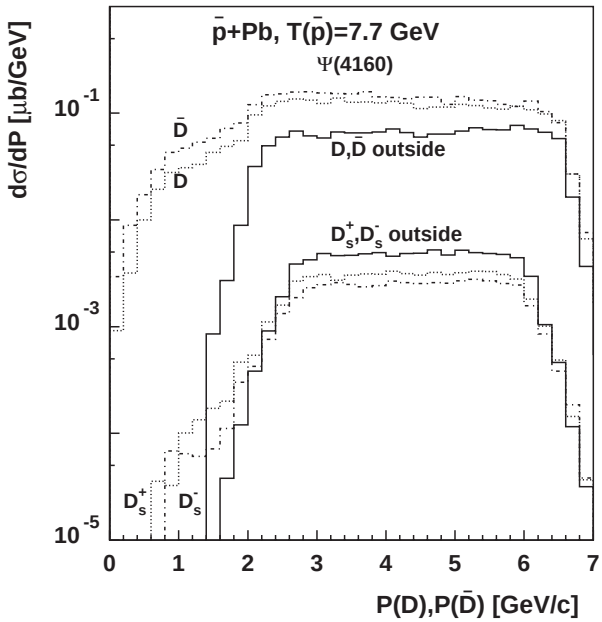

Fig. 8. The calculated momentum distributions of $D, \bar{D}$ (upper lines) and D_s^+, D_s^- (lower lines) mesons for $\bar{p}$ + Pb reactions at $T_{\rm lab} = 7.7$ GeV. The solid lines ($D, \bar{D}$ outside, D_s^+, D_s^- outside) reflect open charm mesons from $\Psi(4160)$ decays in vacuum, the dotted and dash-dotted ($\bar{D}$) lines correspond to resonance decays in the target nucleus, respectively. In the calculations elastic and inelastic scatterings of the $\Psi(4160)$, $D, \bar{D}$ and D_s^+, D_s^- mesons have been taken into account.

the fraction of unscattered $D, \bar{D}$ events. The calculated cross-sections for resonant (l.h.s.) and nonresonant (r.h.s.) production channels are shown in fig. 7 (upper part) for D- and $\bar{D}$-mesons, respectively, as a function of the target mass A at $T_{\rm lab} = 5.7$ GeV. Even for the low-momentum cut the cross-sections are of the order of 50–100 nb for heavy targets, which should be feasible at the HESR with a $\bar{p}$ luminosity of $\sim 2 \times 10^{32}$. The resulting ratio D- to $\bar{D}$-mesons is displayed in the lower part of fig. 7 for resonant (l.h.s.) and nonresonant (r.h.s.) productions separately. The constant line (= 1) results trivially when including charge exchange reactions, however, discarding c-quark exchange reactions. As noted above, the D-meson absorption is larger in the nonresonant case and may reach 40% for the Pb target within the cross-sections specified in sect. 2. Vice versa, experimental data on this ratio (employing the same low-momentum cut) as a function of the mass A will allow to set stringent bounds on the size of the c-quark exchange cross-section in the nuclear medium.

Without explicit representation we note that the perspectives of measuring $D, \bar{D}$ rescattering in heavy nuclei from the resonance decay of the $\Psi(4040)$ are similar to the previous case discussed above and also close to the results for the $\Psi(4160)$ (see below). Since the chances to measure additionally the rescattering effects of D_s^+, D_s^- mesons are very low in view of the small partial decay width for the $\Psi(4040)$ (cf. fig. 1) we directly continue with a discussion of the $\Psi(4160)$ formation and decay at $T_{\rm lab} = 7.7$ GeV.

In this case (for $\bar{p}$ + Pb) the momentum distribution of the $D, \bar{D}, D_s^+, D_s^-$ mesons becomes very broad and extends from ~ 0 to ~ 7 GeV/c (cf. fig. 8) where the "outside" $\Psi(4160)$ decays (solid lines; $D, \bar{D}$ outside, D_s^+, D_s^- outside) give open charm mesons essentially above ~ 2 GeV/c. Thus rescattering events of the D-mesons are dominantly found for momenta less than 2 GeV/c which, unfortunately, are only a low fraction of the total open charm yield. Furthermore, the number of D_s^+, D_s^- events in this low-momentum range is down by more than 2 orders of magnitude relative to the $D, \bar{D}$ mesons. However, apart from the resonant production of charm meson pairs there will be an additional contribution from nonresonant $D, \bar{D}, D_s^+, D_s^-$ mesons which will enhance the cross-section also for low momenta, respectively. It is hard to provide reliable estimates for the nonresonant contribution, but in view of fig. 4 for $T_{\rm lab} = 6.8$ GeV this contribution might be higher by a factor 2–4 than the resonance contribution.

As shown in fig. 9 the cross-sections for $D, \bar{D}$ mesons at $T_{\rm lab} = 7.7$ GeV are above 50 nb for heavy targets (l.h.s, upper part) —even when including a low-momentum cut of 2 GeV/c— showing a sizeable difference due to the absorption of D, D^* mesons in the nucleus. The perspectives for D_s^+, D_s^- mesons are less promising (r.h.s, upper part). Here only cross-sections of ~ 0.1 nb should be expected for a Pb target which might be enhanced due to nonresonant channels by a factor 2–4 (as estimated above). However, the relative absorption of D, D^* mesons —as measured by the ratio to $\bar{D}, \bar{D}^*$ mesons— increases with target mass by

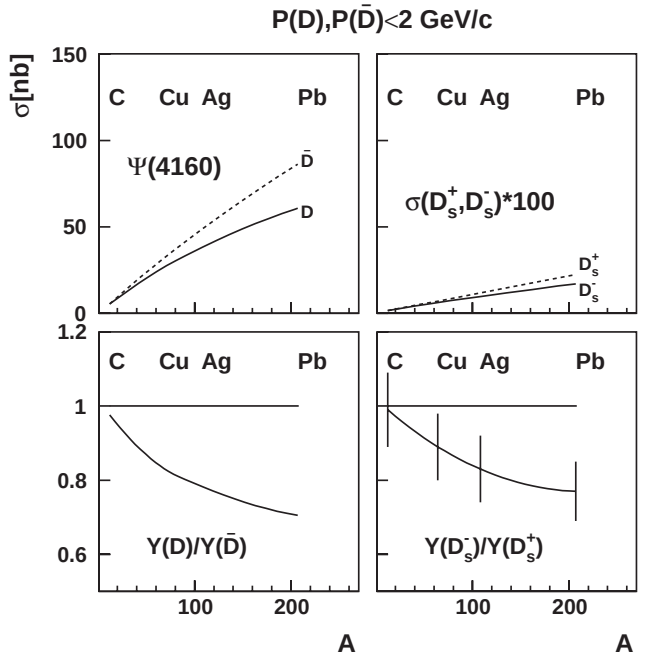

Fig. 9. Upper part: The calculated cross-sections for D- and $\bar{D}$-mesons for $\bar{p}+A$ reactions at $T_{\rm lab}=7.7$ GeV including a low-momentum cut P_D and $P_{\bar{D}} \leq 2.0$ GeV/c. The l.h.s. shows the contribution from in-medium resonance decays for $D, \bar{D}$ whereas the r.h.s. corresponds to D_s^+, D_s^- resonant production (multiplied by a factor 100). Lower part: The ratio $D/\bar{D}$ *versus* the target mass A (l.h.s.) and the ratio D_s^-/D_s^+ for resonant production. The constant line (= 1) results when neglecting s- and c-quark exchange channels.

up to 35% for $A=207$ (l.h.s., lower part) for the cross-sections specified in sect. 2. This decrease in the $D/\bar{D}$ ratio is roughly the same for the $\Psi(4160)$ decays as for the $\Psi(3770)$ decays (fig. 7) inspite of the shorter lifetime of the $\Psi(4160)$. This is partly due to the different cut in momentum and the fact, that the average momentum of the produced $\Psi(4160)$ in the laboratory is higher. The ratio of D_s^-/D_s^+ *versus* target mass A (r.h.s.; lower part) also shows a decrease due to the different cross-sections for c- and s-quark exchanges with the nucleons of the target. The vertical lines in fig. 9 show the statistical error bars in this ratio for the low-momentum cut of 2 GeV/c that reflect the low number of D_s^-, D_s^+ mesons in this momentum range as obtained from the Monte Carlo simulations. In principle, provided that sufficient statistics are obtained experimentally, it is possible to determine the relative strength of (u,d)-, s- and c-quark exchanges with nucleons from the mass dependence of the further ratios D/D_s^+ and D/D_s^-. We only point out this possibility without presenting explicit figures for these ratios since the statistics for $D_s^\pm$ is very small and the cross-sections employed are rather uncertain so far.

5 Summary

In this study we have explored the perspectives of measuring the dynamics of hidden charm vector mesons and open charm mesons in nuclei in antiproton-induced reactions on nuclei. Such experimental studies will be possible at the high-energy antiproton storage ring HESR proposed for the future GSI facility [16]. The Multiple Scattering Monte Carlo (MSMC) calculations performed have been based on the resonance production concept with resonance properties from the PDG [21] or related estimates from high-energy open charm branching ratios. We note, that these resonance properties are in line with $\Psi(3770), \Psi(4040)$ and $\Psi(4160)$ production from e^+e^- annihilation [20], however, the detailed branching ratios for the $\Psi(4040)$ and $\Psi(4160)$ (cf. fig. 1) are still quite uncertain. Thus our estimated uncertainty in the cross-sections is of the order of a factor 2–3, which should be kept in mind when planning experiments along this line. We stress that the total branching ratios to $\bar{p}p$ should be measured first with high accuracy. Deviations from our calculations for hidden charm vector mesons in $\bar{p}p$ reactions than directly carry over to the cross-sections on nuclei (fig. 2). Nevertheless, even for a light nucleus such as ^{12}C cross-sections from 70–150 nb should be expected at the proper resonance energies (fig. 2). Our calculations suggest that the total yield of these vector mesons scales as $\sim A^{0.55}$ with target mass A (fig. 3). For a heavy nucleus like Pb the fraction of "inside" decays to dileptons or $D, \bar{D}$ reaches $\sim$ 50% for the $\Psi(3770)$, $\sim$ 65% for the $\Psi(4040)$ and $\sim$ 75% for the $\Psi(4160)$, which is sufficient to address the question of in-medium properties of these resonances. However, for the rescattering cross-sections adopted in sect. 2, the in-medium modifications of their spectral functions is rather moderate, *i.e.* 15%, 8% and 5% change in width, respectively, such that a mass resolution for dilepton pairs of the order of a few MeV will be necessary. This will be also the case for in-medium mass shifts of these vector mesons which are estimated to be of the order of a few MeV, only [19].

We have, furthermore, explored the perspectives of measuring the interactions of open charm mesons in nuclei that are produced by resonant vector meson decays or nonresonant channels, respectively. For the cross-sections specified in (12) the effects of $D, \bar{D}$ rescattering and D-meson absorption in heavy nuclei can clearly be identified when imposing a low-momentum cut in the laboratory of 2–2.2 GeV/c at $T_{\rm lab}=5.7$ or 7.7 GeV, respectively. This low-momentum cut excludes events with $D\bar{D}$ decays in vacuum or $D, \bar{D}$ mesons that did not rescatter in the target nucleus. The cross-sections for such type of events with D- or $\bar{D}$-mesons of low momenta are of the order of 50 nb for a heavy target like Pb. Such cross-sections are high enough to perform successful experiments with an antiproton luminosity of 2×10^{32} as envisaged for the HESR [16]. Experimentally, the ratio of $D/\bar{D}$ (at low momenta) as a function of target mass A allows to set stringent constraints on the D-meson absorption —or c-quark transfer— cross-section at nuclear density ρ_0. Furthermore, at $T_{\rm lab} \approx 7.7$ GeV the production cross-section of D_s^+, D_s^- mesons should become appreciable and be of the order of 20 nb for a Pb target when including only the $\Psi(4160)$ decays. Approximately 50% of these $(c\bar{s})$ and $(\bar{c}s)$

mesons should rescatter in a target of mass $A \approx 200$ such that c- and s-quark exchange reactions with nucleons can be measured by studying the mass dependence of D_s^-/D_s^+ as well as D/D_s^- and D/D_s^+ at low momenta. However, to exclude events from $\Psi(4160)$ vacuum decays as well as events with unscattered open charm mesons a severe cut on low momenta (≤ 2 GeV) should be performed. In this momentum range the cross-section for D_s^-, D_s^+ drops to ~ 0.1 nb even for a Pb target. It will thus be very hard to measure the various particle ratios as a function of the mass A with good statistics.

We are grateful to A.B. Kaidalov and A. Sibirtsev for helpful discussions and valuable suggestions. Furthermore, we like to thank E.L. Bratkovskaya and U. Wiedner for critical comments and a careful reading of the manuscript. This work was supported by DFG under grant No. 436 RUS 113/600, RFFI and Forschungzentrum Jülich.

References

1. *Quark Matter '96*, Nucl. Phys. A **610**, 1 (1996).
2. *Quark Matter '97*, Nucl. Phys. A **638**, 1 (1998).
3. *Quark Matter '99*, Nucl. Phys. A **661**, 1 (1999).
4. T. Matsui, H. Satz, Phys. Lett. B **178**, 416 (1986).
5. H. Satz, Rep. Progr. Phys. **63**, 1511 (2000).
6. W. Cassing, C.M. Ko, Phys. Lett. B **396**, 39 (1997).
7. W. Cassing, E.L. Bratkovskaya, Phys. Rep. **308**, 65 (1999).
8. R. Vogt, Phys. Rep. **310**, 197 (1999).
9. X.N. Wang, B. Jacak (Editors), *Quarkonium Production in High-Energy Nuclear Collisions* (World Scientific, 1998).
10. K. Haglin, Phys. Rev. C **61**, 031902 (2000).
11. W. Liu, C.M. Ko, Z.W. Lin, Phys. Rev. C **65**, 015203 (2002).
12. B. Müller, Nucl. Phys. A **661**, 272c (1999).
13. J. Hüfner, B.Z. Kopeliovich, Phys. Lett. B **426**, 154 (1998); Y.B. He, J. Hüfner, B.Z. Kopeliovich, Phys. Lett. B **477**, 93 (2000).
14. D. Kharzeev *et al.*, Z. Phys. C **74**, 307 (1997).
15. K. Seth, *Proceedings of the International Workshop Structure of Hadrons, Hirschegg, Austria, Jan. 14-20, 2001*, edited by H. Feldmeier, J. Knoll, W. Nörenberg, J. Wambach (GSI, 2001) p. 183.
16. *An International Accelerator Facility for Beams of Ions and Antiprotons*, `http://www.gsi.de/GSI-Future/cdr/`.
17. W. Cassing, Ye. Golubeva, L.A. Kondratyuk, Eur. Phys. J. A **7**, 279 (2000).
18. S.J. Brodsky, G.A. Miller, Phys. Lett. B **412**, 125 (1997).
19. F. Klingl, S. Kirn, S.H. Lee, P. Morath, W. Weise, Phys. Rev. Lett. **82**, 3396 (1999).
20. J.Z. Bai *et al.*, hep-ex/0102003.
21. Particle Data Group, Eur. Phys. J. C **15**, 1 (2000).
22. W. Cassing, E.L. Bratkovskaya, A. Sibirtsev, Nucl. Phys. A **691**, 753 (2001).
23. Ye. S. Golubeva, A.S. Iljinov, B. Krippa, I.A. Pshenichnov, Nucl. Phys. A **537**, 393 (1992).
24. Ye. S. Golubeva, A.S. Iljinov, I.A. Pshenichnov, Nucl. Phys. A **562**, 389 (1993).
25. W. Cassing, Ye. S. Golubeva, A.S. Iljinov, L.A. Kondratyuk, Phys. Lett. B **396**, 26 (1997).
26. Ye. S. Golubeva, L.A. Kondratyuk, W. Cassing, Nucl. Phys. A **625**, 832 (1997).
27. G.R. Farrar, L.L. Frankfurt, M.I. Strikman, H. Liu, Nucl. Phys. B **345**, 125 (1990).
28. A. Sibirtsev, K. Tsushima, A.W. Thomas, Eur. Phys. J. A **6**, 351 (1999).
29. A. Sibirtsev, Nucl. Phys. A **680**, 274c (2001).
30. A. Hayashigaki, Phys. Lett. B **487**, 96 (2000).
31. Z. Lin, C.M. Ko, Phys. Rev. C **62**, 034903 (2000); J. Phys. G **27**, 617 (2001).
32. A.B. Kaidalov, P.E. Volkovitsky, Z. Phys. C **63**, 517 (1994).